COMMISSIONS 27 AND 42 OF THE IAU
INFORMATION BULLETIN ON VARIABLE STARS

Number 6088

Konkoly Observatory
Budapest
22 December 2013

HU ISSN 0374 – 0676

IDENTIFICATION OF Be AND CARBON STARS IN THE MAGELLANIC CLOUDS AS A BY-PRODUCT OF A SYMBIOTIC STAR SEARCH†

CIESLINSKI, DEONISIO[1]; DIAZ, MARCOS P.[2]; MENNICKENT, RONALD E.[3]; KOŁACZKOWSKI, ZBIGNIEW[4]; PEREIRA, CLÁUDIO B.[5]

[1] Instituto Nacional de Pesquisas Espaciais, Divisão de Astrofísica, Brazil

[2] Instituto de Astronomia, Geofísica e Ciências Atmosféricas, Universidade de São Paulo, Brazil

[3] Depto. de Astronomía, Universidad de Concepción, Chile

[4] Astronomical Institute, University of Wrocław, Poland

[5] Observatório Nacional, Rio de Janeiro, Brazil

Symbiotic stars are a sub-group of interacting binaries consisting of a cool giant which transfers material via stellar wind or Roche-lobe overflow to a hot and compact object which is thought to be a white dwarf or even, in a few cases, a neutron star. The optical spectra show the presence of a continuum with TiO and/or VO absorption bands, eventually Swan bands, absorption lines of neutral and singly ionized metals (from the cool star) and emission lines of the Balmer series, HeI, [OIII] as well as emission lines of high ionization species such as HeII and [FeVII], which are associated with the surrounding nebula and/or an accretion disc. Photometrically they present variability on several time scales, from minutes to several decades with amplitudes from a few thousandths to several magnitudes. The orbital periods are ranging from ∼200 days to several years or even decades. Reviews on symbiotic stars can be found in Friedjung & Viotti (1982), Kenyon (1986), Mikołajewska et al. (1988), Mikołajewska (1997), Corradi, Mikołajewska & Mahoney (2003) and Mikołajewska & Szczerba (2007).

Nowadays, about 200 symbiotic stars are known, see e.g., the catalog of Belczyński et al. (2000). This catalog contains 188 objects confirmed as true symbiotics and 30 as suspected. Surprisingly, however, among the confirmed symbiotics only 8 are in Large Magellanic Cloud and 6 in the Small Magellanic Cloud, with half of them harboring carbon stars. It is a known fact that the physical condition driving the symbiotic phenomenon depends on several factors, the surface metallicity of the cool star being one of them (see, e.g., the discussion of Jorissen 2003). In this sense, one may expect qualitative differences between the population of symbiotics in our Galaxy and those in the Magellanic Clouds. Unfortunately, the sample of symbiotics in the LMC and SMC is far too small to enable any statistical comparison with the population of symbiotics in our Galaxy. In addition, the proposed evolutionary link between Super-Soft X-Ray Sources (SSS) and symbiotic systems in the Clouds still depends on a better knowledge of the symbiotic population in

†This paper includes data gathered with the 6.5 meter Magellan Telescopes located at Las Campanas Observatory, Chile and with the Southern Astrophysical Research (SOAR) telescope, which is a joint project of the Ministério da Ciência, Tecnologia, e Inovação (MCTI) da República Federativa do Brasil, the U.S. National Optical Astronomy Observatory (NOAO), the University of North Carolina at Chapel Hill (UNC), and Michigan State University (MSU).

this environment, where the population of SSS is much better defined than in our Galaxy (e.g., Kahabka 1997). Such a comparison may help us to understand the evolutionary links between symbiotics, supersoft X-ray sources, type Ia supernovae, and the metallicity-dependent mechanisms of mass loss in those binaries. This fact motivated us to design and conduct a search program aiming at discovering and confirming new symbiotic binaries in these nearby galaxies.

The fact that symbiotic stars present spectral and photometric peculiarities provides us with several ways of discovering them, i.e., we can find candidates to this class using published photometric and/or spectroscopic data. Consequently, targets can be selected among objects with peculiar colors (e.g., presence of UV excess with red colors with respect to normal stars), light curve peculiarities (e.g., eruptions or large-amplitude irregular variations) and among catalogues of objects with emission lines. In fact, we have discovered some new symbiotic stars during a photometric and spectroscopic survey on L-, I- and IS-type irregular variables (Cieslinski et al. 1994, 1997).

In this work the targets were selected using combined criteria comprising their color, photometric variability and the presence of emission lines. Our first step was to define the intrinsic color region for known symbiotics with M-type giants in our Galaxy using data from the literature (Munari et al. 1992 and Munari & Jurdana-Sepic 2002; see also Henden & Munari 2008) (Fig. 1). Such a wide region reflects the presence of a red continuum with an enhanced UV/blue emission. A large number (10^5) of potential targets, corrected for extinction towards the LMC and SMC, were selected, above the three dashed segments of Fig. 1, from the photometric *UBVI* surveys of Zaritsky et al. (2002, 2004). The long lists were further constrained by the typical absolute magnitude range of symbiotics with giant primaries (usually brighter than a G5 giant) based on the LMC/SMC distance moduli. Those are still numerous samples with contamination from binaries and normal stars with similar color indices. These lists were then cross-correlated with the OGLE and MACHO variable stars database, yielding a few hundred targets. Known variables were removed from our lists. Finally, the light curves of the LMC candidates were visually inspected, searching for photometric variability that would be consistent with those of a photometrically active symbiotic stars. The observation priority for the LMC targets was defined by the morphology of their MACHO light curves. A different strategy was adopted for the SMC for which three emission line object catalogs are publicly available (Meyssonnier & Azzopardi 1993, Murphy & Bessell 2000 and Evans et al. 2004). The cross-correlation of the photometrically selected sample with the emission line sources yields a list with 90 candidates.

The observations reported in this contribution were performed from 2004 to 2009 with the Magellan Clay 6-m LDSS-31 and the SOAR 4.1-m GOODMAN spectrograph (Clemens et al. 2004). The spectral resolution obtained is ∼0.7 nm and ∼0.2 nm for the SOAR and Magellan spectra, respectively. The spectral coverage of the individual spectra is indicated in column 7 of Tables 1 and 2. Relative flux calibration was performed in arbitrary units on all Magellan spectra. In this case, the relative flux calibration was attempted by applying an average extinction curve and a sensitivity function estimated by comparing the spectra of observed B stars with literature SEDs having the same spectral type (Jacoby et al. 1984). An approximate absolute flux calibration was performed on the SOAR data by using an average extinction curve and the observations of one or two tertiary spectrophotometric standard stars from Hamuy et al. (1994) per night. Absolute calibration errors are estimated to be smaller than 0.2 mag for the SOAR data. Thin cirrus clouds were present during the Magellan observations while photometric conditions

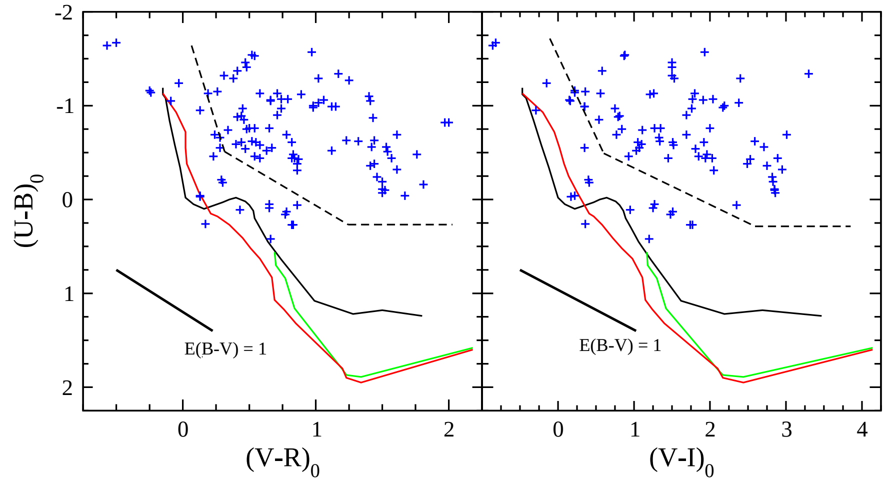

Figure 1. Color diagrams for known symbiotic stars in the Galaxy, corrected for interstellar extinction (blue pluses). Approximante reddening corrections were computed using the galactic extinction model by Amôres & Lépine (2005) and a few values from literature, when available. The black, red and green curves show the main-sequence, supergiant and giant colors, respectively. Reddening vectors are plotted in the lower left corners. The straight dashed lines represent our initial selection criteria and were used to select objects from the photometric *UBVI* surveys of Zaritsky et al. (2002, 2004). Additional photometric and/or spectroscopic criteria were applied to this subsample to finally obtain our candidate lists for the LMC and the SMC.

prevailed for most of the SOAR science exposures. The wavelength-calibration exposures were taken before or after the target exposures. However, the SOAR spectra may include small (few times the FWHM resolution) wavelength shifts and should not be used for deriving radial velocities. All the reduction of the spectroscopic data was done with the IRAF package[1].

The log of the observations is listed in Table 1 (Be stars) and Table 2 (carbon stars). In these tables, column 1 gives the file name of the spectrum, columns 2 and 3 are the coordinates of the object, column 4 indicates the Heliocentric Julian Day of the middle of the exposure, column 5 is the exposure time in seconds, column 6 gives the signal to noise ratio of the spectrum, column 7 shows the spectral coverage in nm, column 8 gives the OGLE and/or MACHO identification (if any), while the numbers in column 9 indicate the comments on individual objects, cited in the footnotes of these tables.

Several Be and carbon stars were found in our sample. The applied selection criteria plus the presence of emission lines in the SMC targets proved to be effective in selecting carbon and Be stars. This small but homogeneously selected sample comprises both types of objects in the LMC and SMC. Carbon stars were identified by the presence of a red continuum with Swan bands in the optical region (e.g., in 438.2, 473.7, 516.5, 563.6 and 619.1 nm). We classified the target as a carbon star if one or more of these bands were present. The identification of the Be stars was performed by considering the presence of a blue continuum with at least one emission line of the Balmer series (generally, Hα). Some objects also show other emission lines such as HeI, FeII, CaII triplet at 849.8, 854.2 and

[1]IRAF is distributed by the National Optical Astronomy Observatories, which are operated by the Association of Universities for Research in Astronomy, Inc., under cooperative agreement with the National Science Foundation.

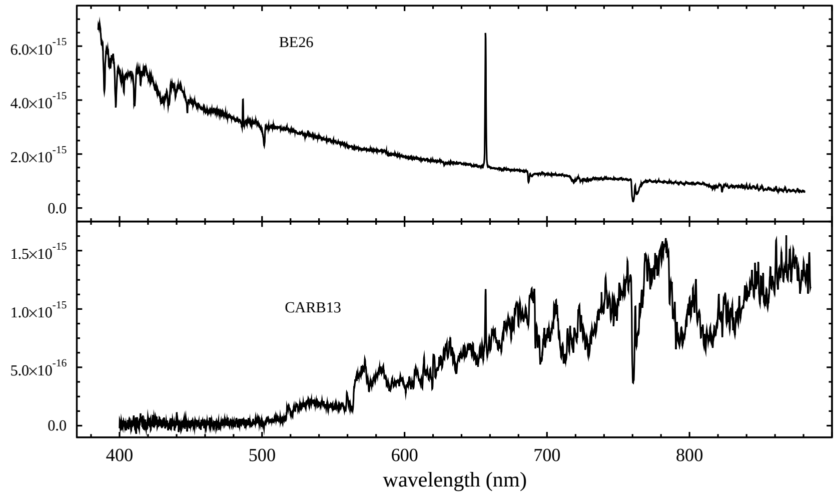

Figure 2. Sample spectra of Be stars (top) and carbon stars (bottom). Flux units are erg cm^{-2} s^{-1} $Å^{-1}$.

866.2 nm, OI in 777.2 and 844.6 nm and some lines of Paschen series. Six objects with 'flat' continuum and/or objects in which the flux calibration is more uncertain (mainly the ones observed with Magellan Clay telescopes) were classified as Be or Ce candidates.

A brief description of the main spectroscopic characteristics of each individual object is given in the notes of Tables 1 and 2. Sample spectra for both classes can be seen in Fig. 2. All the spectra (in ASCII format) are accessible in the auxiliary files 6088-d1.tar.gz and 6088-d2.tar.gz.

Some objects, however, appear to be more interesting and deserve more detailed investigation. Among them, we mention the carbon stars with indications of a blue continuum that might indicate binarity, and the objects with a 'flat' continuum. From the data at hand we conclude that most of the carbon stars we found are cool. Nevertheless, a precise classification of the sample of carbon stars may require additional observations. Among the Be stars some objects present HeI and FeII emission lines. Absorption line reversals are also seen in some objects. Metallicity effects are important in the evolution of carbon stars and also for the mass loss mechanism feeding the circumstellar disks of Be stars. Statistical comparison of controlled samples in our Galaxy and in the Clouds may help to improve our knowledge on these objects.

Acknowledgements. MPD thanks CNPq grant #305175. We also thank the anonymous referee for his/her comments and suggestions.

References:

Amôres, E. B., Lépine, J. R. D., 2005, *AJ*, **130**, 659

Belczyński, K., Mikołajewska, J., Munari, U., Ivison, R. J., Friedjung, M., 2000, *A&AS*, **146**, 407

Cieslinski, D., Elizalde, F., Steiner, J. E., 1994, *A&AS*, **106**, 243

Cieslinski, D., Steiner, J. E., Elizalde, F., Pereira, M. G., 1997, *A&AS*, **124**, 57

Clemens, J. C., Crain, J. A., Anderson, R., 2004, *Proc. SPIE*, **5492**, 331

Corradi, R. L. M., Mikołajewska, J., Mahoney, T. J., eds., 2003, *ASP Conference Series*, Vol. **303**
Evans, C. J., Howarth, I. D., Irwin, M. J., Burnley, A. W., Harries, T. J., 2004, *MNRAS*, **353**, 601
Friedjung, M., Viotti, R., eds., 1982, *IAU Coll.*, **70**, 45
Hamuy, M., Suntzeff, N. B., Heathcote, S. R., Walker, A. R., Gigoux, P., Phillips, M. M., 1994, *PASP*, **106**, 566
Henden, A., Munari, U., 2008, *Baltic Astronomy*, **17**, 293
Jacoby, G. H., Hunter, D. A., Christian, C. A., 1984, *ApJS*, **56**, 257
Jorissen, A., 2003, *ASP Conference Series*, **303**, 25
Kahabka, P., 1997, *ARA&A*, **35**, 69
Kenyon, S. J., 1986, *The Symbiotic Stars*, Cambridge University Press, Cambridge
Meyssonnier, N., Azzopardi, M., 1993, *A&AS*, **102**, 451
Mikołajewska, J., Friedjung, M., Kenyon, S. J., Viotti, R., eds., 1988, *IAU Coll.*, **103**
Mikołajewska, J., ed., 1997, *Physical Processes in Symbiotic Binaries and Related Systems*, Copernicus Foundation for Polish Astronomy, Warsaw
Mikołajewska, J., Szczerba R., eds., 2007, *Evolution and Chemistry of Symbiotic Stars, Binary Post-AGB and Related Objects*, *Baltic Astronomy*, **16**, No.1, 1-164
Munari, U., Yudin, B. F., Taranova, O. G., Massone, G., Marang, F., Roberts, G., Winkler, H., Whitelock, P. A., 1992, *A&AS*, **93**, 383
Munari, U., Jurdana-Sepic, R., 2002, *VizieR Online Data Catalog*, 338
Murphy, M. T., Bessell, M. S., 2000, *MNRAS*, **311**, 741
Zaritsky, D., Harris, J., Thompson, I. B., Grebel, E. K., Massey, P., 2002, *AJ*, **123**, 855
Zaritsky, D., Harris, J., Thompson, I. B., Grebel, E. K., 2004, *AJ*, **128**, 1606

Table 1: Be stars and candidates

File name	α_{2000}	δ_{2000}	HJD (2450000+)[a]	Exp. Time (s)	S/N[b]	Sp. coverage (nm)	Other names[c]	Notes
be01.txt	00:43:05.3	−72:35:48.8	4710.8560	51	24.78	385−880		1
be02.txt	00:46:41.7	−73:22:53.8	4683.8808	60	44.79	460−890		2
be03.txt	00:47:01.4	−73:26:46.0	4792.6039	600	44.37	385−880		3
be04a.txt	00:48:23.7	−73:15:29.1	4710.7503	50	29.48	385−880	OGLE004823.67−731528.9	4
be04b.txt	”	”	4301.7712	360	73.50	530−815	”	”
be04c.txt	”	”	4301.7712	360	72.39	375−528	”	”
be05.txt	00:48:34.9	−73:17:53.6	4710.6959	38	21.49	385−880		5
be06a.txt	00:48:43.0	−73:03:10.9	4301.7818	420	70.35	530−815		6
be06b.txt	”	”	4301.7818	420	24.52	375−528		”
be07.txt	00:49:29.8	−72:56:01.2	3339.6529	200	19.64	380−704	OGLE004929.80−725550.0/208.15910.39	7
be08.txt	00:49:38.0	−73:06:10.0	4710.6166	30	17.79	385−880		8
be09.txt	00:49:55.7	−73:07:35.0	4709.8495	34	14.71	385−880		9
be10a.txt	00:50:14.8	−73:05:55.8	4301.7016	360	69.13	530−815	OGLE005014.80−730555.8	10
be10b.txt	”	”	4301.7016	360	38.67	375−528	”	”
be11a.txt	00:52:06.5	−73:18:18.9	4301.7380	360	109.27	530−815	OGLE005206.37−731818.7	11
be11b.txt	”	”	4301.7380	360	37.81	375−528	”	”
be11c.txt	”	”	4734.7926	120	25.66	385−880	”	”
be12.txt	00:52:13.0	−72:31:46.4	4708.8664	30	22.63	385−880		12
be13.txt	00:52:31.0	−73:13:38.7	4710.6674	34	17.42	385−880		13
be14a.txt	00:52:52.6	−73:18:33.7	4301.7129	360	76.85	530−815	OGLE005252.49−731833.5	14
be14b.txt	”	”	4301.7129	360	173.38	375−528	”	”
be15a.txt	00:54:21.2	−73:16:31.5	4301.7610	420	100.60	530−815	OGLE005421.16−731631.5	15
be15b.txt	”	”	4301.7610	420	27.73	530−815	”	”
be15c.txt	”	”	4734.8167	180	34.57	375−528	”	”
be16a.txt	00:54:41.2	−72:27:54.4	4301.7512	420	46.50	530−815	OGLE005441.15−722754.5	16
be16b.txt	”	”	4301.7512	420	98.19	375−528	”	”
be16c.txt	”	”	4734.8341	240	3.12	385−880	”	”
be17.txt	00:54:42.0	−73:45:50.3	4734.8642	240	31.05	385−880		17
be18a.txt	00:56:40.0	−72:45:23.7	4301.6853	300	120.50	530−815	OGLE005639.94−724523.9	18
be18b.txt	”	”	4301.6853	300	133.91	375−528	”	”
be18c.txt	”	”	4709.8898	30	32.09	385−880	”	”
be19.txt	00:57:24.5	−71:44:52.2	4708.9020	36	43.55	385−880		19
be20.txt	00:58:45.2	−72:36:51.8	4709.7735	200	7.91	385−880		20
be21.txt	00:58:58.3	−72:28:53.1	4710.6398	30	8.78	385−880		21
be22.txt	01:05:42.7	−72:27:46.7	4709.8071	34	30.85	385−880		22
be23.txt	01:15:45.9	−73:20:39.8	4734.8037	180	32.70	385−880		23
be24.txt	01:17:09.0	−73:17:09.0	4710.7226	50	34.40	385−880		24
be25.txt	05:04:52.3	−69:54:43.6	4803.7147	600	35.22	385−880		25
be26.txt	05:15:27.2	−68:54:03.3	4836.7415	550	74.75	385−880		26
be27.txt	05:22:02.7	−69:46:14.6	4803.6572	450	49.92	405−880	OGLE052202.89−694614.6	27
be28.txt	05:25:35.8	−69:47:26.4	4795.7735	600	85.76	385−880	OGLE052536.74−694726.4	28
be29.txt	05:27:21.4	−69:22:57.0	4834.7113	300	62.77	385−880	OGLE052721.71−692257.1	29
be30.txt	05:28:45.0	−69:21:18.0	4795.7515	600	105.25	385−880	OGLE052845.28−692117.9	30
be31.txt	05:35:43.6	−69:09:30.9	4835.6047	400	38.29	385−880		31

a) HJD of the middle of the exposition
b) S/N was measured redward of Hα (or Hβ for data in the blue)
c) OGLE/MACHO name
1) Blue continuum + Hα and Hβ in emission (FeII 523.5 and HeI 587.6 nm in emission?)
2) Flat continuum + Hα in emission; CaII triplet (849.8, 854.2 and 866.2 nm) in absorption → Be or Ge?
3) Flat continuum + Hα and Hβ in emission (HeI 587.6 nm in emission?); CaII triplet in absorption (HeI 501.6 nm in absorption?, G Band in 430.0 nm?) → Be or Ge?
4) Blue continuum + Hα, Hβ and Hγ in emission
5) Blue continuum + Hα and Hβ in emission (HeI 587.6 nm and HeI 706.5 nm in emission?)
6) Blue continuum(?) + Hα and Hβ in emission (HeI 587.6 nm in emission?) → Be?
7) Blue continuum + Hα in emission; the other Balmer lines are in absorption
8) Blue continuum + Hα in emission; Hδ and Hϵ in absorption
9) Blue continuum + Hα in emission (Hβ and HeI 587.6 nm in emission?); Hγ and Hδ in absorption
10) Blue continuum(?) + Hα in emission; the other Balmer lines are in absorption → Be?
11) Flat continuum + Hα and Hβ in emission → Be or Ge?
12) Blue continuum + Hα in emission; the other Balmer lines are in absorption
13) Blue continuum + Hα, Hβ, HeI 587.6, HeI 667.8 and HeI 706.5 nm in emission
14) Blue continuum(?) + Hα and Hβ in emission → Be?
15) Weak blue continuum + Hα and Hβ in emission (Hβ with P Cygni profile in JD 2454301.5)
16) Blue continuum + Hα and Hβ in emission (Hβ with emission core in JD 2454301.5); the other Balmer lines and HeI in 402.6 and 447.1 nm are in absorption
17) Blue continuum + Hα and Hβ in emission (Hβ with P Cygni profile?); Hδ and Hγ in absorption (with emission core?)
18) Blue continuum + Hα, Hβ, HeI 587.6, HeI 667.8 and HeI 706.5 nm in emission (Hβ with P Cygni profile in JD 2454301.5); the other Balmer lines are in absorption; emission in ∼393.8 nm (CIII/FeII or artifact?), ∼464.5 nm (CIII/NIII or arfifact?) and ∼674.5 nm (CIII or artifact?)
19) Blue continuum + Hα in emission; the other Balmer lines and CaII triplet are in absorption
20) Blue continuum + Hα and Hβ in emission
21) Blue continuum + Hα, Hβ, HeI 587.6, HeI 667.8(?) and HeI 706.5 nm in emission
22) Blue continuum + Hα, Hβ, HeI 587.6, HeI 667.8 and HeI 706.5 nm in emission; Hϵ, Hδ and Hγ in absorption
23) Blue continuum + Hα, Hβ, Hγ, FeII (417.3, 417.8, 435.2, 516.9, 531.7 and 553.5 nm), CaII triplet and OI 844.6 nm in emission
24) Blue continuum + Hα in emission; the other Balmer lines are in absorption (emission core in Hγ?); CaII triplet in absorption
25) Blue continuum + Hα and Hβ in emission (OI 844.6 nm in emission?); the other Balmer lines are in absorption (CaII triplet in absorption?)
26) Blue continuum + Hα, Hβ (with emission core) and FeII (516.9, 519.8 and 531.7 nm) in emission (CaII triplet and some lines of Paschen series in emission?); H8+HeI 388.9, Hϵ, Hγ, HeI(402.6, 414.5, 438.7, 447.1, 492.2 and 501.6 nm) in absorption
27) Blue continuum + Hα and Hβ in emission; Hδ and Hγ in absorption (CaII triplet and some lines of Paschen series in emission?)
28) Blue continuum + Hα in emission (Hβ with emission core?; HeI in 587.6 and 706.5 nm, CaII triplet and some lines of Paschen series in emission?); Hϵ, Hδ, Hγ and HeI 501.6 nm in absorption
29) Blue continuum + Hα, Hβ, Hγ (with emission core), HeI 587.6, HeI 667.8, HeI 706.5, OI 777.2, OI 844.6 nm and some lines of Paschen series in emission
30) Blue continuum + Hα, Hβ, Hγ (with emission core), HeI 587.6 and HeI 706.5 nm in emission (CaII triplet and some lines of Paschen series in emission?); Hϵ, Hδ (emission core?) and HeI 501.6 nm in absorption
31) Blue continuum + Hα and Hβ in emission (OI 844.6 nm in emission?); Hγ in absorption

Table 2: Carbon stars

File name	α_{2000}	δ_{2000}	HJD (2450000+)[a]	Exp. Time (s)	S/N[b]	Sp. coverage (nm)	Other names[c]	Notes
carb01.txt	00:37:22.2	−73:22:25.0	3339.5371	200	7.38	379−704	OGLE003722.15−732222.8/213.15162.5	1
carb02.txt	00:40:14.2	−72:49:59.2	4792.5573	600	4.50	400−886		2
carb03.txt	00:42:15.3	−72:57:29.6	3340.5535	200	8.92	383−704	OGLE004216.08−725731.9/213.15453.10	3
carb04.txt	00:44:56.5	−73:12:25.7	3339.5865	200	7.10	379−704	OGLE004456.46−731224.2/212.15621.153	4
carb05.txt	00:50:58.5	−73:00:03.4	3340.5802	200	17.09	383−704	OGLE005058.90−730006.6/212.16023.42	5
carb06.txt	00:51:06.6	−73:05:09.2	3339.6705	200	9.34	379−704	OGLE005106.53−730502.8/212.16021.35	6
carb07.txt	00:55:17.4	−72:57:37.2	3339.7391	200	2.28	379−704	OGLE005516.51−725733.4/211.16308.19	7
carb08.txt	00:58:35.1	−72:59:31.9	3340.6092	300	21.03	383−704	OGLE005835.16−725935.4/211.16479.2	8
carb09.txt	00:59:29.1	−72:39:24.7	3340.6245	300	8.90	383−704	OGLE005929.08−723926.7/207.16541.11	9
carb10.txt	01:08:47.3	−72:40:16.6	3340.6585	200	1.90	383−704	OGLE010846.90−724019.4/206.17168.79	10
carb11.txt	05:05:16.5	−68:44:44.3	3339.7479	100	5.77	379−704	OGLE050515.90−684446.6/1.4056.1146	11
carb12a.txt	05:06:49.1	−69:51:41.7	4302.9302	300	22.04	530−815		12
carb12b.txt	"	"	4302.9302	300	19.36	375−528		"
carb13.txt	05:11:25.1	−69:47:03.7	4836.6489	500	12.91	400−884		13
carb14.txt	05:11:40.7	−68:48:15.3	3339.7555	100	15.78	379−704	OGLE051139.99−684816.8/79.5023.40	14
carb15a.txt	05:11:59.0	−68:43:01.7	4301.9438	300	18.34	530−815		15
carb15b.txt	"	"	4301.9438	300	11.05	375−528		"
carb16.txt	05:16:10.3	−69:35:19.1	3339.8446	200	8.77	379−704	OGLE051609.74−693517.9/78.5737.19	16
carb17a.txt	05:16:44.7	−69:27:47.3	4302.8806	300	25.77	530−815		17
carb17b.txt	"	"	4302.8806	300	30.92	375−528		"
carb18.txt	05:18:10.5	−69:26:20.7	3340.7342	300	20.21	383−704	OGLE051810.88−692626.5/78.6102.490	18
carb19.txt	05:19:53.9	−69:27:55.8	3340.7680	300	4.40	383−704	OGLE051954.02−692802.8/78.6465.85	19
carb20.txt	05:19:58.3	−69:14:09.4	3340.7808	300	2.58	383−704	OGLE051958.26−691416.7/80.6468.77	20
carb21.txt	05:20:47.3	−69:50:38.8	3340.7982	300	2.68	383−704	OGLE052047.00−605046.2/78.6580.62	21
carb22.txt	05:21:54.6	−70:56:49.0	3340.8095	200	9.28	383−704	OGLE052154.24−705657.0/13.6685.29	22
carb23.txt	05:25:55.8	−69:43:52.9	3339.7669	200	3.18	379−704	OGLE052555.11−6945354.1/77.7429.64	23
carb24.txt	05:28:18.8	−70:05:23.1	4795.7236	600	1.46	400−886	OGLE052818.82−700523.1	24
carb25.txt	05:36:09.3	−70:22:19.6	3339.7761	100	3.67	379−704	OGLE053608.58−702220.5/11.8992.23	25
carb26.txt	05:39:00.6	−69:52:24.5	3339.7876	200	7.56	379−704	OGLE053900.00−695225.1/81.9484.20	26
carb27.txt	05:42:23.7	−70:18:01.6	3340.8424	300	10.52	383−704	OGLE054223.01−701810.3/12.100821.100	27
carb28.txt	05:44:34.5	−70:39:48.2	3339.8070	200	15.05	379−704	OGLE054433.79−703949.1/12.10440.10	28
carb29.txt	05:46:58.9	−70:25:04.9	3339.8168	200	9.44	379−704	OGLE054658.32−702505.6/12.10807.15	29

a) HJD of the middle of the exposition
b) S/N was measured in the continuum between 450 and 540 nm
c) OGLE/MACHO name
1) Swan bands in 438.2, 473.7, 516.5 and 563.6 nm
2) Weak Swan bands in 563.6 and 619.1 nm
3) Swan bands in 473.7, 516.5 and 563.6 nm + weak Hα in emission
4) Swan bands in 438.2, 473.7, 516.5 and 563.6 nm
5) Swan bands in 473.7, 516.5 and 563.6 nm
6) Swan bands in 438.2, 473.7, 516.5 and 563.6 nm
7) Swan bands in 473.7, 516.5 and 563.6 nm (the bumps below 450.0 nm is artifact?)
8) Swan bands in 516.5 and 563.6 nm + presence of a blue continuum below of 465 nm → binary star?
9) Swan bands in 438.2, 473.7, 516.5 and 563.6 nm
10) Swan bands in 516.5 and 563.6 nm + Hα in emission
11) Swan bands in 473.7, 516.5 and 563.6 nm
12) Swan bands in 516.5, 563.6 and 619.1 nm
13) Swan bands in 516.5 and 563.6 nm + Hα in emission
14) Swan bands in 473.7, 516.5 and 563.6 nm + Hα and Hβ in emission
15) Swan bands in 516.5, 563.6 and 619.1 nm
16) Swan bands in 516.5 and 563.6 nm + Hα in emission, weak blue continuum below of 500 nm? → binary star?
17) Swan bands in 473.7, 516.5 and 563.6 nm
18) Swan bands in 516.5 and 563.6 nm + Hα in emission + weak blue continuum with the other Balmer lines in absorption → binary star?
19) Swan bands in 473.7, 516.5 and 563.6 nm + weak Hα in emission
20) Swan bands in 516.5 and 563.6 nm + weak Hα in emission
21) Swan bands in 516.5 and 563.6 nm
22) Swan bands in 473.7, 516.5 and 563.6 nm
23) Swan bands in 473.7, 516.5 and 563.6 nm
24) Swan bands in 516.5 and 563.6 nm
25) Swan bands in 438.2, 473.7, 516.5 and 563.6 nm
26) Swan bands in 516.5 and 563.6 nm
27) Swan bands in 516.5 and 563.6 nm + weak Hα in emission
28) Swan bands in 473.7, 516.5 and 563.6 nm + weak Hα in emission
29) Swan bands in 473.7, 516.5 and 563.6 nm + weak Hα in emission